CHAPTER VI
MORPHOLOGY AND PHOTOPHYSICAL PROPERTIES OF ELECTROSPUN LIGHT-EMITTING POLYSTYRENE/ POLYFLUORENE DERIVATIVE FIBERS

6.1 Abstract

Electrospun (e-spun) fibers of poly(2,7-(9,9-bis(2-ethylhexyl)fluorene)) (BEH-PF) blended with polystyrene (PS) with average diameters ranging from 0.68 to 1.04 μm were successfully prepared. Electrospinnability of the PS/BEH-PF solution was improved by the addition of a volatile organic salt, pyridinium formate (PF), to the solution prior to electrospinning. Scanning electron microscopy (SEM) and Fourier-transformed infrared spectroscopy (FT-IR) were respectively used to observe morphology and chemical integrity of the e-spun fibers. Additionally, absorption and emission of the as-prepared solution and its corresponding e-spun products, spin-coated and solution-cast films were investigated by UV-Visible (UV-Vis) and photoluminescence (PL) spectroscopy. Both of the e-spun products (beads and fibers) exhibited a red shift in their emission spectra, when compared with those of the solutions. It is due to the aggregation of BEH-PF molecules occurring from the π-π interaction stacking and resulting in the decreasing HOMO-LUMO energy gap as the lower energy emission peaks observed. Interestingly, the different morphological appearances also directly affect their color emissions.

(**Key-words**: Electrospinning; Polyfluorene; Phophysical properties)

6.2 Introduction

The electrospinning (e-spinning) process is a very potential method for fabricating ultra-fine fibers with diameters in the nanometer to sub-micrometer range.[1, 2] In the e-spinning process, a high electrical potential is used to create an electrically charged jet of polymer solution which dries or solidifies to deposit a polymer fiber on the collector. One electrode is placed into the spinning solution and the other electrode is attached to a collector. The electrical field is subjected to the end of a capillary tube that contains the polymer fluid held by its surface tension. This induces a charge on the surface of the polymer fluid.[3, 4] Then, the charge repulsion also causes a force directly opposite to the surface tension. This force tends to elongate a hemispherical surface of the fluid at the end of capillary tube form a conical shape known as the Taylor cone as the applied electrical potential increases.[3-5] And this is what makes a continuous flow of the polymer jet shot to the collector. Due to the combination of many forces on the polymer jet, the jet will be shot as a straight line where either splitting or bending instability can be also occurred. Finally, during its flight to the collector the charged jet thins down and, at the same time, it dries out or solidifies leaving ultra-fine fibers on the collector where random orientation is usually observed. Because the e-spinning is a very simple, inexpensive and high throughput continuous production method, thus many researchers have studied the e-spinning of various materials such as biopolymers, conductive polymers, block copolymers, polymer blends, ceramics, and composite materials.[3-8]

In the recently decade, conductive polymers have been widely explored both in chemical and physical properties for various applications. Polyfluorene and its derivatives are one of the most interesting conductive polymers. Due to electronic and optical properties such as high electro- and photoluminescence efficiencies with emission wavelengths in the green to blue color region [9, 10] that can be applied in various electronic devices such as an organic light-emitting device (OLED) [11, 12], and solar cell [13].

Since previous studies on this class of materials usually focused on the properties of either the solutions or the films thereof, it is of our interest to

investigate the possibility for fabricating these polymers into ultra-fibrous form that exhibits a high surface area to volume or mass ratio that could be applied as a small-scale electronic and optoelectronic device in the future.

Recently, Kuo and coworkers [14] successful prepared light-emitting electrospun (e-spun) nanofibers of the binary blends of poly(methyl methacrylate) (PMMA) and polyfluorene derivatives (e.g. poly(9,9-dioctylfluoreny-2,7-diyl) (PFO), poly[2,7-(9,9-dihexylfluorene)-*alt*-5,8-quinoxaline] (PFQ), poly[2,7-(9,9-dihexylfluorene)-*alt*-4,7-(2,1,3-benzothiadiazole)] (PFBT), and poly[2,7-(9,9-dihexylfluorene)-*alt*-5,7-(thieno[3,4-b]pyrazine)] (PFTP)). The uncontinuous fiberlike structure was obtained at the low PFO/PMMA blend ratio but became a core-shell structure at a high PFO blend ratio. The full color light-emitting e-spun nanofibers could be fabricated from the binary blends of polyfluorene derivative/PMMA as the uniform e-spun fibers produced from the binary blends of PFO/PMMA, PFQ/PMMA, PFBT/PMMA, and PFTP/PMMA exhibited the color emission of blue, green, yellow, and red, respectively. After that, Chen and some of previous Kuo's coworkers [15] further fabricated the full color e-spun nanofibers based on ternary blends of PFO/poly[2-methoxy-5-(2-ethylhexyloxy)- 1,4-phenylenevinylene] (MEH-PPV)/PMMA. They found that PFO/MEH-PPV ratio directly affects the morphology and photophysical properties according to the energy transfer between these two polymers.

In the present work, the e-spinning was used as the technique for fabricating other type of polyfluorene derivatives which is poly(2,7-(9,9-bis(2-ethylhexyl)fluorene)) (BEH-PF) into ultra-fine fibers. Polystyrene (PS) was used as the matrix material into BEH-PF which BEH-PF was blended. Chloroform was used as the common solvent. Morphological appearance and chemical integrity of the e-spun fibers were evaluated, while photophysical properties such as absorption and emission directly related to its morphology appearances of the PS/BEH-PF solution and its corresponding e-spun fibers were also studied. Moreover the spin-coated and solution-cast films of PS/BEH-PF blend also produced for using as references.

6.3 Experimental

6.3.1 Materials and Preparation of Solutions for Spinning and Casting Films

Poly(2,7-(9,9-bis(2-ethylhexyl)fluorene)) (BEH-PF) ($M_n \approx 3.2 \times 10^4$ Daltons) which its chemical structure is shown in Figure 6.1 was synthesized following the procedure described in reference [16]. Polystyrene (PS) ($M_w \approx 3.0 \times 10^5$ Daltons, pellets form) was a general purpose grade from Dow Chemicals (USA). The solvent used was chloroform (CF; Carlo Erba, Italy). Pyridinium formate (PF), an volatile organic salt, was prepared by the reacting an equimolar quantity of pyridine (Lab-Scan (Asia), Thailand) and formic acid (Merck, England). Blend solutions of 8.5% (w/v) PS/BEH-PF in CF (the compositional weight ratio between PS and BEH-PF being 7.5:1) with or without the addition of 8% (v/v) PF were prepared.

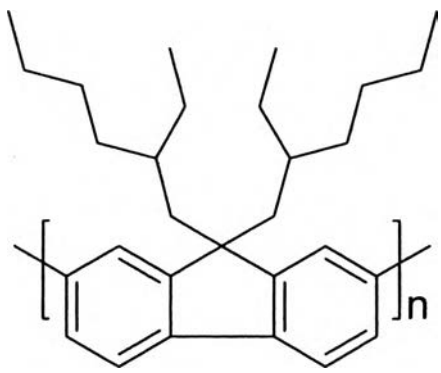

Figure 6.1 Chemical structure of poly(2,7-(9,9-bis(2-ethylhexyl)fluorene)) (BEH-PF).

6.3.2 Electrospining

Blend solutions were carried out for e-spinning under an applied electrical potential, ranging between 7.5 and 20 kV. Both the collection distance and the collection time were fixed at 10 cm and 1 min, respectively. Each of the as-prepared solutions was placed in a 5 ml plastic syringe, the open end of which was

connected to a blunt-ended stainless steel gauge 20 needle (the outside diameter = 0.91 mm), used as the nozzle. An aluminum sheet wrapped around a hard plastic sheet used as a backing plate was used as the collector plate. The emitting electrode of positive polarity from a Gamma High-Voltage Research ES30P DC power supply (Florida, USA) was connected to the needle, while the grounding electrode was connected to the collector plate. The feed rate of the solution was controlled by means of a Kd Scientific syringe pump at 1 $mL \cdot h^{-1}$.

6.3.3 Spin-Coating and Solution-Casting

The spin coating and solution casting methods were used to prepare the films of that PS/BEH-PF blend solution in CF. In details, the spin coating was done on a glass slide by Specialty Coating Systems model P6700 with the spinning speed of 1,000 rpm to get a final thickness of 0.5-1 μm. Solution casting was also done on a glass slide and the resulted thickness is about 1-2 μm.

6.3.4 Characterizations

Morphological appearance of the as-spun products was examined by a JEOL JSM-5410LV scanning electron microscope (SEM). Diameters of the e-spun fibers were measured directly from SEM images of 1,000× magnification, with the average value being calculated from at least 50 measurements (for each spinning condition). The average bead diameters and the number of beads per unit area (i.e., the bead density) on the e-spun beaded fibers were calculated from measurements on SEM images of 500× magnification. A Thermo-Nicolet Nexus 670 Fourier-transformed infrared spectroscope (FT-IR) was used to characterize the as-received PS pellets, the as-synthesized BEH-PF, and some of the e-spun products. Lastly, absorption spectra and photoluminescence emission spectra of the PS/BEH-PF solutions in CF with or without PF addition, the corresponding e-spun products, spin-coated and solution- cast films were measured by a Hewlett Packard-8254A diode array UV-VIS spectrophotometer (UV-Vis) and Perkin- Elmer LS50 luminescence spectrometer (PL), respectively. Each sample was excited at 350 nm prior to measurement for PL measurement.

6.4 Results and discussion

6.4.1 Morphology of the E-spun Fibers Spun from PS/BEH-PF and PS/BEH-PF Added PF Solutions

Figure 6.2 shows selected SEM images of e-spun products at various applied electrical potential (e.g., 7.5, 10, 12.5, 15, 17.5 and 20 kV) from 8.5% (w/v) solutions of PS/BEH-PF (PS:BEH-PF = 7.5:1) in chloroform (CF) without and with 8% (v/v) pyridinium formate (PF). It is obvious that the discrete beads were observed for the neat PS/BEH-PF solution as shown in series (a) of Figure 6.2 with the average diameter and bead density ranging from 14.65 to 23.05 μm and 0.34×10^5 to 2.10×10^5 beads·cm^{-2} respectively. (see in Table 6.1 which shows average fiber diameters, bead size and bead density of e-spun products from 8.5% (w/v) solutions of PS/BEH-PF in CF without and with 8% (v/v) PF at various applied electrical potential)

Upon the addition of PF into the PS/BEH-PF solutions (see series (b) in Figure 6.2), the ultra-fine fibers were obtained with the average diameter ranging from 0.68 to 1.04 μm were obtained (see in Table 6.1). These results consistent with the previous and other publications that the addition of PF into the solutions before e-spinning successfully improves the e-spinnability of the solutions as the disappearance of beads in the e-spun product was found due to the significant increase in the total number of charges carried within the jet [4, 17, 18]. Moreover, the average diameter of the e-spun fibers was found to increase with increasing the applied electrical potential, (see in Table 6.1), a direct result of the increase in the total number of charged species within a jet segment that causes both the electrostatic forces to increase. These, in turn, could result in an increase in the actual feed rate of the solution as well as a decrease in the total path trajectory of the jet segment, due to an increase in the speed of the jet [18, 19].

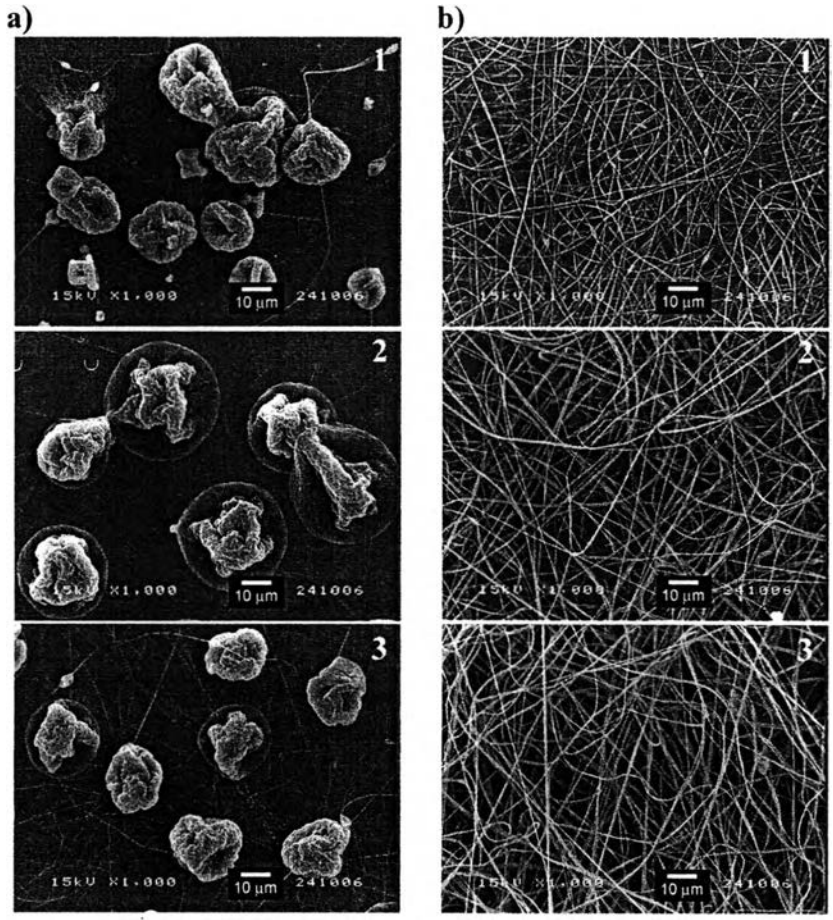

Figure 6.2 Selected SEM images (1000×; scale bar = 10 µm) of the electrospun products from 8.5% (w/v) solutions of PS/BEH-PF (PS:BEH-PF = 7.5:1) in chloroform (CF) without a) and with b) 8% (v/v) pyridinium formate (PF), at applied electrical potential (1) 7.5, (2) 10, (3) 12.5, (4) 15, (6) 17.5 and (6) 20 kV. The collection distance, collection time and solution flow rate were fixed at 10 cm, 1 min, and 1 $mL \cdot h^{-1}$, respectively.

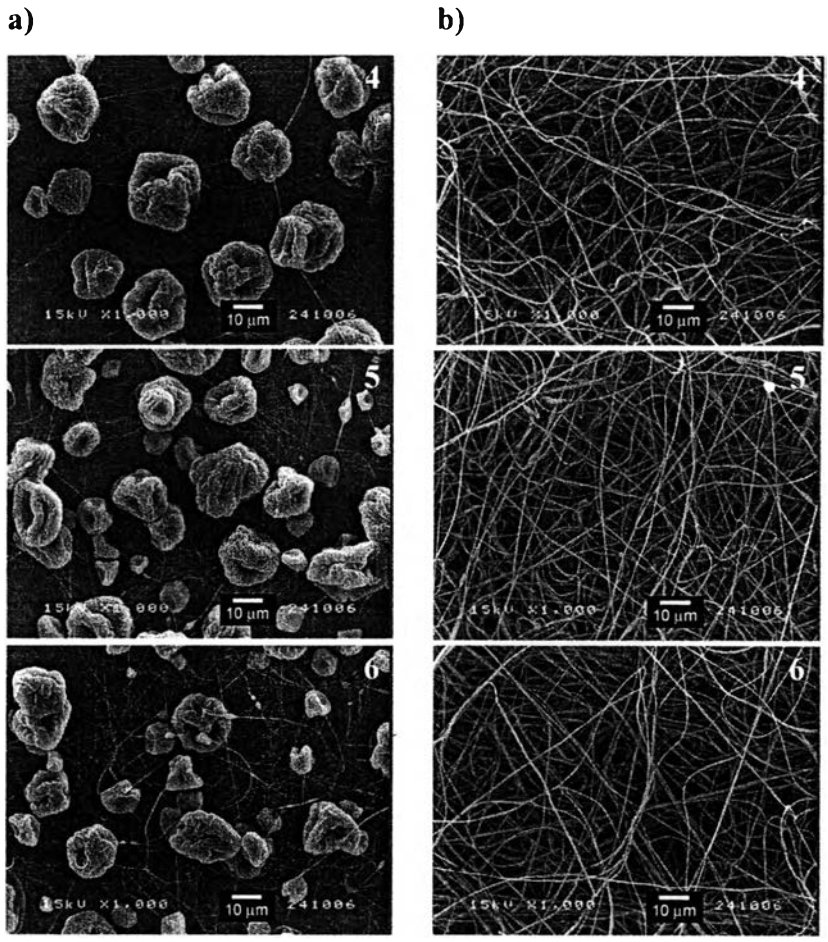

Figure 6.2 (Cont.) Selected SEM images (1000×; scale bar = 10 μm) of the electrospun products from 8.5% (w/v) solutions of PS/BEH-PF (PS:BEH-PF = 7.5:1) in chloroform (CF) without a) and with b) 8% (v/v) pyridinium formate (PF), at applied electrical potential (1) 7.5, (2) 10, (3) 12.5, (4) 15, (6) 17.5 and (6) 20 kV. The collection distance, collection time and solution flow rate were fixed at 10 cm, 1 min, and 1 $mL \cdot h^{-1}$, respectively.

Table 6.1 Average fiber diameters, bead size and bead density of the electrospun products from 8.5% (w/v) solutions of PS/BEH-PF (PS:BEH-PF = 7.5:1) in chloroform (CF) without and with 8% (v/v) pyridinium formate (PF) at various applied electrical potential. The collection distance, collection time and solution flow rate were fixed at 10 cm, 1 min, and 1 $mL \cdot h^{-1}$, respectively

Solution	HV (kV)	Fiber Diameters (μm)	Bead Size (μm)	Bead Density (# bead·cm^{-2})
PS/BEH-PF /CF	7.5	-	14.65 ± 6.19	0.40×10^5
	10.0	-	23.05 ± 11.25	0.34×10^5
	12.5	-	19.14 ± 5.64	0.78×10^5
	15.0	-	16.11 ± 4.09	1.18×10^5
	17.5	-	16.80 ± 4.29	2.02×10^5
	20.0	-	14.05 ± 5.79	2.10×10^5
PS/BEH-PF /CF+ PF	7.5	0.68 ± 0.16	-	-
	10.0	0.79 ± 0.19	-	-
	12.5	0.85 ± 0.23	-	-
	15.0	0.92 ± 0.19	-	-
	17.5	0.98 ± 0.15	-	-
	20.0	1.04 ± 0.17	-	-

6.4.2 Chemical Integrity of E-spun Fibers Spun from PS/BEH-PF, and PS/BEH-PF Added PF Solutions

To confirm the PS and BEH-PF component in the e-spun products by Figure 6.3, which shows the IR spectra (in the wavenumber range of 500-4000 cm^{-1}) of the of PS pellet, BEH-PF powder and some of the e-spun products from 8.5% (w/v) solutions of PS/BEH-PF in CF without and with the presence of PF at applied electrical potential 15 kV. The chemical functionalities of the e-spun products from 8.5% (w/v) PS/BEH-PF solutions in CF without and with the presence of PF were compared with those obtained from the as-received PS pellets and the as-synthesized

BEH-PF. Table 6.2 summarizes some absorbance peaks characteristic of the PS and BEH-PF component in the e-spun products. According to Figure 6.3, the peaks characteristic of PS component were evident in all of the FT-IR spectra of the as-spun fibers (e.g., at 696-698, 1,490, and 3,020-3,030 cm^{-1}). Moreover, the peaks characteristic of BEH-PF are 813 and 1,380 cm^{-1} which belongs to CH out-of-plane bending vibrations in $C=CH_2$ group and CH bending vibrations in CH_3 deformation, respectively. Additionally, the peak at 2,850 and 2,920 cm^{-1} are specific to symmetric CH stretching vibrations in $-CH_2$ group and asymmetric CH stretching vibrations in $-CH_2$ group, respectively. These results indicate that PS and BEH-PF still exist in the e-spun products and no change in their chemical structure.

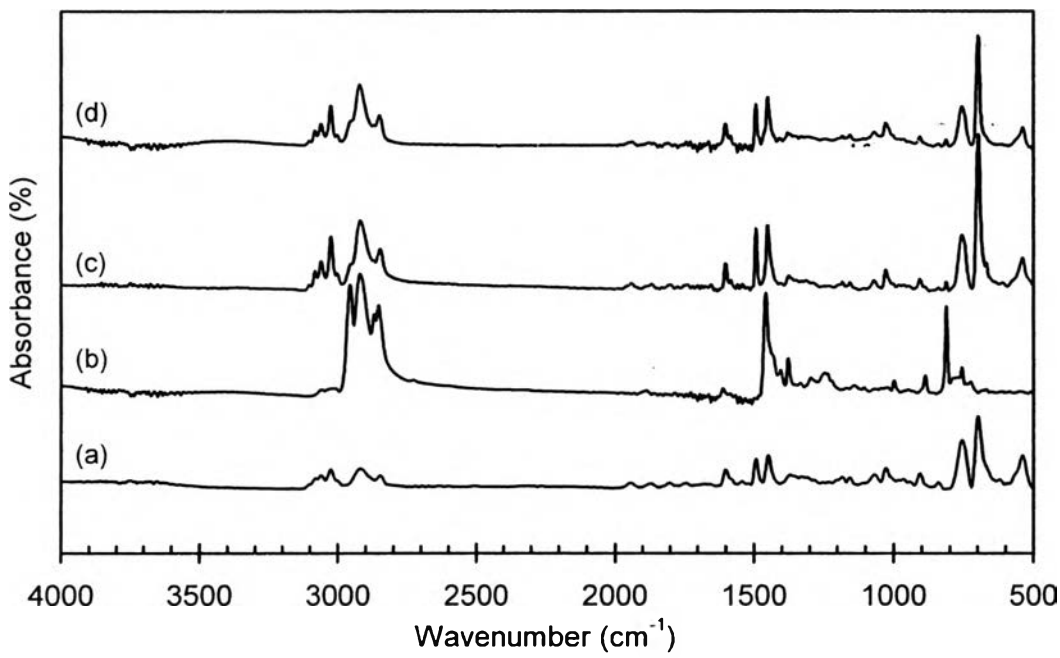

Figure 6.3 IR spectra of a) PS pellet, b) BEH-PF powder and the electrospun products from 8.5% (w/v) solutions of PS/BEH-PF (PS:BEH-PF = 7.5:1) in chloroform (CF) without c) and with d) 8% (v/v) pyridinium formate (PF) at applied electrical potential 15 kV. The collection distance, collection time and solution flow rate were fixed at 10 cm, 1 min, and 1 $mL \cdot h^{-1}$, respectively.

Table 6.2 Analysis of IR spectra of as-received PS pellet, BEH-PF powder and the electrospun products from 8.5% (w/v) solutions of PS/BEH-PF (PS:BEH-PF = 7.5:1) in chloroform (CF) without and with 8% (v/v) pyridinium formate (PF) at applied electrical potential 15 kV. The collection distance, collection time and solution flow rate were fixed at 10 cm, 1 min, and 1 $mL \cdot h^{-1}$, respectively

As-received materials (cm^{-1})		Electrospun products (cm^{-1})		Assignment
PS	BEH-PF	PS/ BEH-PF /CF	PS/ BEH-PF /CF + PF	
698	-	696	698	CH bending vibrations in CH deformation
754	756	756	756	CH out-of-plane bending vibrations in -CH=CH-(cis) group
-	813	813	813	CH out-of-plane bending vibrations in $C=CH_2$ group
906	886	906	906	CH out-of-plane bending vibrations in $-CH=CH_2$ group
-	1380	1380	1380	CH bending vibrations in $-CH_3$ deformation
1450	1460	1450	1450	Asymmetric CH bending vibrations in $-CH_3$ group
1490	-	1490	1490	CH bending vibrations in CH_2 Scissoring group
1600	1610	1600	1600	C=C stretching vibrations in Conjugated
2850	2850	2850	2850	Symmetric CH stretching vibrations in $-CH_2$ group
2920	2920	2920	2920	Asymmetric CH stretching vibrations in $-CH_2$ group
-	2960	-	-	Asymmetric CH stretching vibrations in $-CH_3$ group
3030	-	3020	3020	CH stretching vibrations in =C-H, $=CH_2$ and CH group
3060	-	3060	3060	CH stretching vibrations in =C-H, $=CH_2$ and CH group

6.4.3 Optical Properties of the Spinning Solutions, E-spun Fibers, and Spin-coated and Solution-cast Reference Films

To further study the photophysical properties (e.g. absorption and emission) of the as-prepared solution, their e-spun products, spin-coated and solution-cast films, UV-Visible (UV-Vis) and photoluminescence (PL) spectroscopy were used to investigate. All spectra results were normalized for clarity. Figure 6.4(a) shows the absorption spectra of the PS/BEH-PF solutions with or without the presence of PF (all spectra results were normalized for clarity). Apparently, the maxima of both spectra were observed at the same value (i.e., 384 nm). Additionally, Figure 6.4(b) shows the emission patterns of the PS/BEH-PF solutions with or without the presence of PF. For both types of the solutions, a sharp peak was observed at 416 nm, with a shoulder being observed at 436 nm, corresponding to the violet-blue color emission of BEH-PF. The relaxation of excited π-electrons to different vibrational energy levels of electronic ground state as corresponded to the violet-blue color emission of the solutions. Evidently, the addition of PF into the base PS/BEH-PF solution did not affect both the absorption and the emission spectra of the resulting solution at all. These characteristics of the absorption and emission spectra correspond to the intrinsic nature of conjugated polymers which have chromophores with various conjugation lengths.[20, 21] Because of the random twisting of main chain prevents the delocalization of π-electrons throughout the entire polymeric molecule, according to the specific optical properties of these individual chromophores such as chain conformation, energy levels, HOMO-LUMO energy gap and emission efficiency.[21-26]

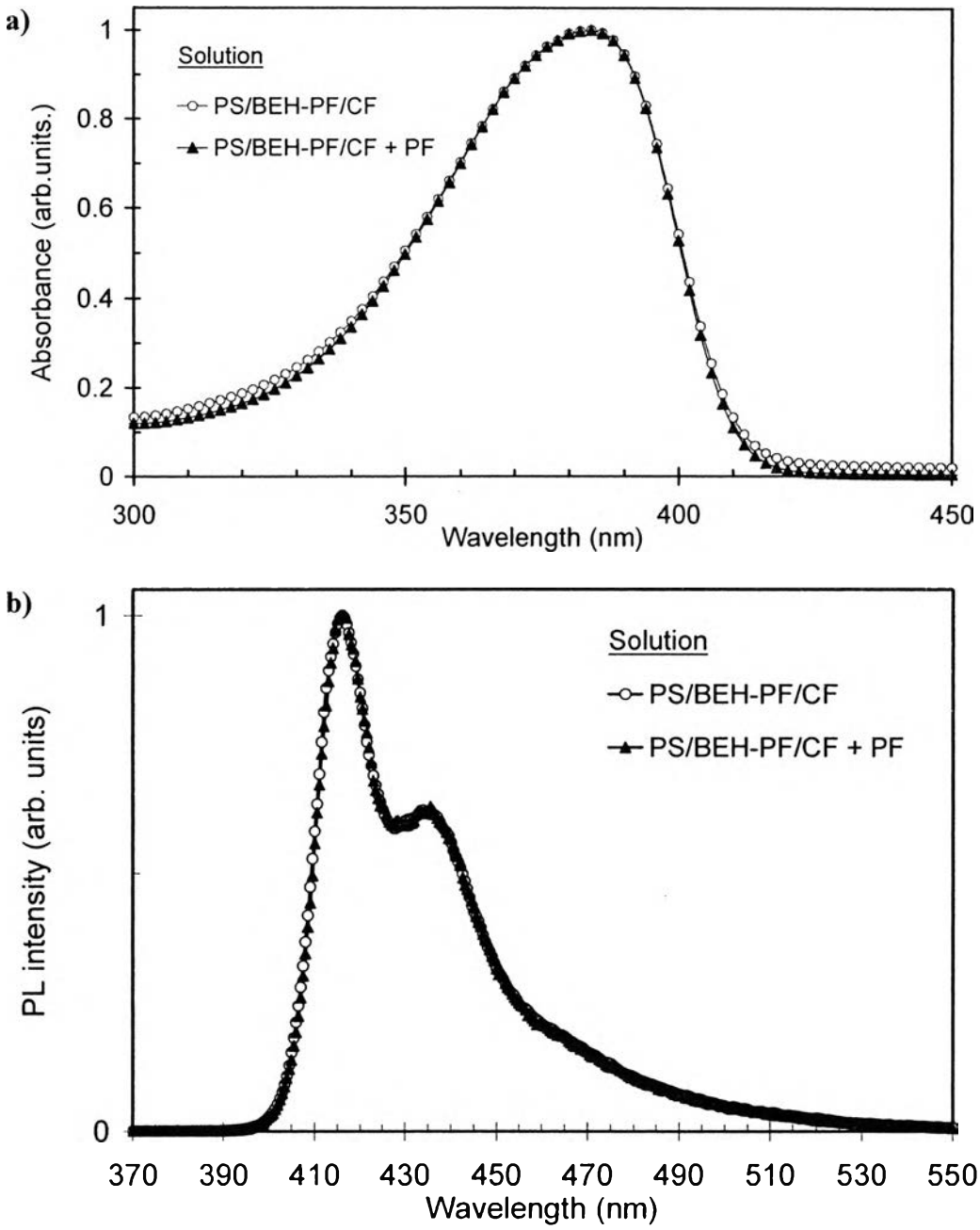

Figure 6.4 a) Absorption and b) PL emission spectra of 8.5% (w/v) solutions of PS/BEH-PF (PS:BEH-PF = 7.5:1) in chloroform (CF) without and with 8% (v/v) pyridinium formate (PF).

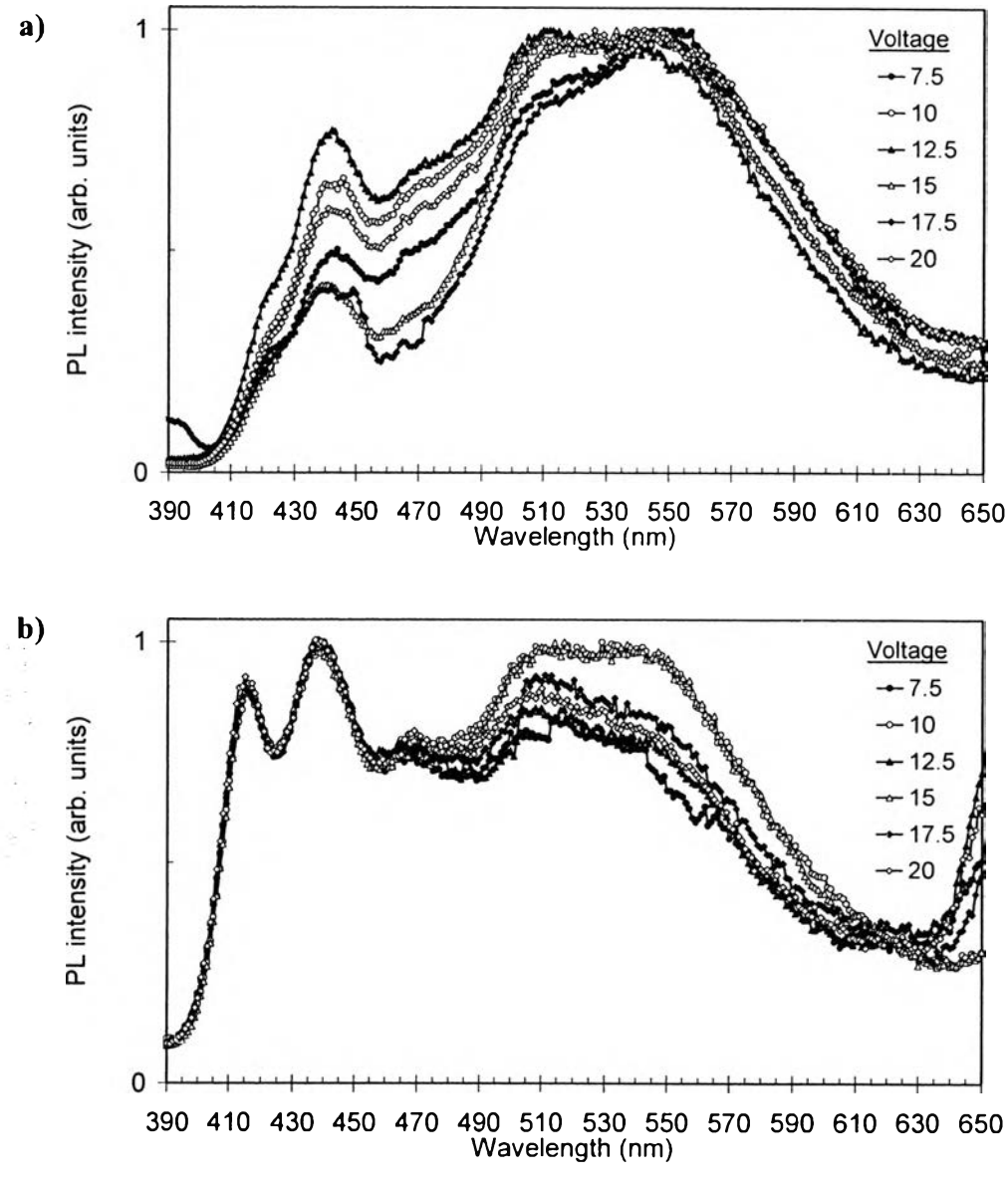

Figure 6.5 PL Emission spectra of the electrospun products spun from 8.5% (w/v) solutions of PS/BEH-PF (PS:BEH-PF = 7.5:1) in chloroform (CF) without a) and with b) 8% (v/v) pyridinium formate (PF) at various applied electrical potential.

With regards to the emission of the e-spun products, it is obvious that the morphology of the e-spun products significantly affected their emission spectra as shown in Figure 5(a) and (b) which show the emission spectra of the e-spun products spun from 8.5% (w/v) solutions of PS/BEH-PF in CF without and with 8 vol.-% PF, respectively, as a function of the applied electrical potential. All emission

spectra of the discrete beads exhibit a peak centered around 530 nm and shoulder centered around 442 nm, while the peaks and shoulder of the e-spun fibers are around 439 (1^{st} maximum intensity), 417 (2^{nd} maximum intensity), and 536 nm, respectively. In addition, both of the e-spun products exhibited a red shift in their emission spectra, when compared with those of the solutions, possibly due to the aggregation of BEH-PF in both types of the e-spun products as lower energy emission peaks were observed. The aggregation of BEH-PF chains occurred from the π-π interaction stacking provides the increased number of energy levels of the individual chromophores, resulting in the longer conjugation length arrangement conformations of BEH-PF chains and then the decreasing HOMO-LUMO energy gap of those individual chromophores occurred. [20, 21, 27-30] Moreover, there is no clear relationship between the emission peak positions and the applied electrical potential as both kinds of the e-spun products exhibit minor differences (see Figure 6.5(a) and (b)). It seem to suggest that the fluctuation in the forces (e.g. gravitational force, surface tension, electrostatic force, Coulombic repulsion force, viscoelastic force and drag force) [4, 17, 18, 31] acting on BEH-PF molecules within jet segments during e-spinning.

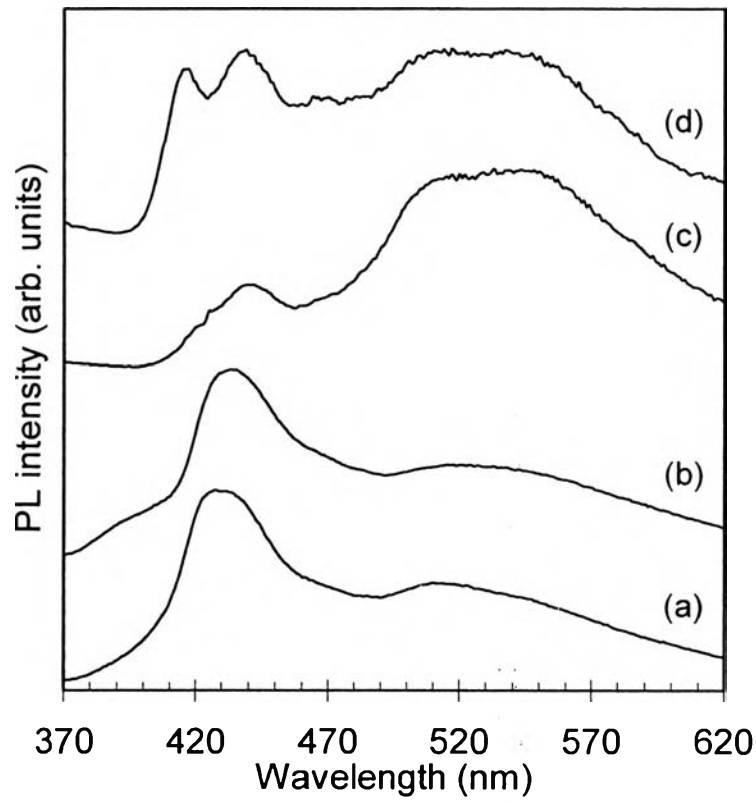

Figure 6.6 PL Emission spectra of samples produced from solutions of 8.5% (w/v) solutions of PS/BEH-PF (PS:BEH-PF = 7.5:1) in chloroform (CF). Samples were a) spin-coated film, b) solution-cast film, the electrospun (e-spun) c) beads, and d) fibers at applied electrical potential 15 kV.

To further study in more details of PL emission characteristics, the films produced by spin coating and solution casting from solutions of 8.5% (w/v) solutions of PS/BEH-PF (PS:BEH-PF = 7.5:1) in CF were also investigated for comparison with both kinds of the e-spun products (see figure 6.6). The summary of the positions and color emission of peak and shoulders in the PL emission spectra of those samples is shown in Table 6.3. The PL emission pattern of the spin-coated film exhibit a maximum emission centered around 430 nm and shoulders centered around 515 nm. For the solution-cast film, its emission peak is at about 435 nm and shoulder is at about 522 nm. Both kinds of films also exhibit a red shift in their emission spectra corresponding to the blue-green color emission, when compared with those

of the solutions, due to the aggregation of BEH-PF molecules as discussed previously.

Table 6.3 Summary of the positions and color emission of peak and shoulders in the PL emission spectra of 8.5% (w/v) solutions of PS/BEH-PF (PS:BEH-PF = 7.5:1) in chloroform (CF) without and with 8% (v/v) pyridinium formate (PF), the corresponding spin-coated and solution-cast films, and the electrospun (e-spun) products (beads and fibers) at applied electrical potential 15 kV

Sample	Peak and Shoulders (nm)			Color Emission
	Violet	Blue	Green	
Solutions	*416	+436	-	Violet-Blue
Spin-coated film	-	*430	+515	Blue-Green
Solution-cast film	-	*435	+522	Blue-Green
E-spun beads	-	+442	*530	Green-Blue
E-spun fibers	**417	*439	+536	Blue-Violet-Green

* = peak with the 1st maximum intensity

* * = peak with the 2nd maximum intensity

\+ = shoulder

To consider the peak position of PL emission spectra of all samples (see Table 6.3), the e-spun beads show a much more red shift than e-spun fibers, solution-cast and spin-coated films, respectively. Interestingly, the e-spun fibers only illustrate the emission peak at the higher energy region (wavelength around 416 nm) similar to the as-prepared solution. Looking closely at the color emission of the e-spun products, the e-spun beads show the green-blue color emission while the e-spun fibers exhibit the blue-violet-green color emission. It can be concluded that the different morphological appearances significantly affect their color emissions.

6.5 Conclusions

We successful prepared the electrospun (e-spun) fibers with average diameters ranging from 0.68 to 1.04 μm of poly(2,7-(9,9-bis(2-ethylhexyl)fluorene)) (BEH-PF) with polystyrene (PS) from the blend solution of 8.5% (w/v) PS/BEH-PF in chloroform (CF) (the compositional weight ratio between PS and BEH-PF being 7.5:1). Electrospinnability of the PS/BEH-PF solution was improved by the addition of a volatile organic salt, pyridinium formate (PF), to the solution prior to electrospinning as the bead formation disappeared. From FT-IR results of the chemical structure study which indicate that PS and BEH-PF still exist in the e-spun products and no change in their chemical structure. The photophysical properties study shows that the blend solutions exhibit the violet-blue color emission. Additionally, both of the e-spun products (beads and fibers) exhibited a red shift in their emission spectra, when compared with those of the solutions as the green-blue and blue-violet-green color emissions, respectively, observed. This is due to the aggregation of BEH-PF molecules occurring from the π-π interaction stacking. Thus the decrease in HOMO-LUMO energy gap of individual chromophores of BEH-PF was obtained which correspond to their photophysical properties. However, both kinds of films (spin-coated and solution-cast films) also showed the red shift in their emission patterns as we observed the blue-green color emission for both types of film fabrication. It seems to be concluded that the different morphological appearances significantly affect to the color emission. This study leads to application of various morphological materials in a small-scale electronic and optoelectronic devices such as OLED and solar cell which require the full range color and various types of HOMO-LUMO energy gap.

6.6 Acknowledgments

The authors acknowledge partial support received from (a) the Thailand Research Fund (TRF) (through a research career development grant: RMU4980045), (b) the National Center of Excellence for Petroleum, Petrochemicals, and Advanced

Materials (NCE-PPAM), and (c) the Petroleum and Petrochemical College (PPC), Chulalongkorn University. SC acknowledges a doctoral scholarship received from the Royal Golden Jubilee PhD Program, the Thailand Research Fund (TRF).

6.7 References

[1] Y. C. Ahn, S. K. Park, G. T. Kim, Y. J. Hwang, C. G. Lee, H. S. Shin, J. K. Lee, Curr Appl Phys 2006, 6, 1030.

[2] N. Dharmaraj, C. H. Kim, K. W. Kim, H. Y. Kim, E. K. Suh, Spectrochimica Acta Part A 2006, 64, 136.

[3] Z. M. Huang, Y. Z. Zhang, M. Kotaki, S. Ramakrishna, Compos Sci Technol 2003, 63, 2223.

[4] P. Wutticharoenmongkol, P. Supaphol, T. Srikhirin, T. Kerdcharoen, T. Osotchan, J Polym Sci Part B Polym Phys 2005, 43, 1881.

[5] Y. Wu, J. Y. Yu, J. H. He, Y. Q. Wan, Chaos Solitons and Fractals 2007, 32, 5.

[6] X. Li, X. Hao, D. Xu, G. Zhang, S. Zhong, H. Na, D. Wang, J Membrane Sci 2006, 281, 1.

[7] S. Tungprapa, I. Jangchud, P. Ngamdee, M. Rutnakornpituk, P. Supaphol, Mater Lett 2006, 60, 2920.

[8] H. Wang, X. Lu, Y. Zhao, C. Wang, Mater Lett 2006, 60, 2480.

[9] A. M. Assaka, P. C. Rodrigues, A. R. M. Oliveira, L. Ding, B. Hu, F. E. Karasz, L. Akcelrud, Polymer 2004, 45, 7071.

[10] J. Liu, G. Tu, Q. Zhou, Y. Cheng, Y. Geng, L. Wang, D. Ma, X. Jing, F. Wang, J Mater Chem 2006, 16, 1431.

[11] V. N. Bliznyuk, S. A. Carter, J. C. Scott, G. Klaırner, R. D. Miller, D. C. Miller, Macromolecules 1999, 32, 361.

[12] H. Lee, A. R. Johnson, J. Kanicki, IEEE Transactions Electron Dev 2006, 53, 427.

[13] T. Yohannes, F. Zhang, M. Svensson, J. C. Hummelen, M. R. Andersson, Q. Inganäs, Thin Solid Films 2004, 449, 152.

[14] C. C. Kuo, C. H. Lin, W. C. Chen, Macromolecules 2007, 40, 6959.

[15] H. C. Chen, C. T. Wang, C. L. Liu, Y. C. Liu, W. C. Chen, J Polym Sci Part B Polym Phys 2009, 47, 463.

[16] U. Scherf, E. J. W. List, Adv Mater 2002, 14, 477.

[17] C. Mit-uppatham, M. Nithitanakul, P. Supaphol, Macromol Chem Phys 2004, 205, 2327.

[18] S. Chuangchote, T. Srikhirin, P. Supaphol, Macromol Rapid Commun 2007, 28, 651.

[19] H. Fong, I. Chun, D. H. Reneker, Polymer 1999, 40, 4585.

[20] J. Kim, T. M. Swager, Nature 2001, 411, 1030.

[21] P. F. Barbara, A. J. Gesquiere, S. J. Park, Y. Lee, J Acc Chem Res 2005, 38, 602.

[22] G. Padmanaban, S. Ramakrishnan, J Am Chem Soc 2000, 122, 2244.

[23] J. L. Brédas, D. Beljonne, V. Coropceanu, J. Cornil, Chem Rev 2004, 104, 4971.

[24] G. Padmanaban, S. Ramakrishnan, J Phys Chem B 2004, 108, 14933.

[25] R. Traiphol, N. Charoenthai, T. Srikhirin, T. Kerdcharoen, T. Osotchan, T. Maturos, Polymer 2007, 48, 813.

[26] R. Traiphol, T. Srikhirin, T. Kerdcharoen, T. Osotchan, N. Scharnagl, R. Willumeit, Eur Polym J 2007, 43, 478.

[27] T. Q. Nguyen, I. B. Martini, J. Liu, B. J. Schwartz, J Phys Chem B 2000, 104, 237.

[28] A. Menon, M. Galvin, K. A. Walz, L. Rothberg, Synth Met 2004, 141, 197.

[29] Q. Chu, Y. Pang, Macromolecules 2005, 38, 517.

[30] S. R. Amrutha, M. Jayakannan, J Phys Chem B 2006, 110, 4083.

[31] L. Wannatong, A. Sirivat, P. Supaphol, Polym Int 2004, 53, 1851.